

JHK Standard Stars for Large Telescopes: the UKIRT Fundamental and Extended Lists.

Timothy G. Hawarden^{1,5*}, S. K. Leggett¹, Michael B. Letawsky^{1,2,3},
David R. Ballantyne^{1,2,4} & Mark M. Casali⁵

¹ Joint Astronomy Centre, 660 N. A‘ohoku Place, Hilo, Hawaii 96720, USA

² Department of Physics and Astronomy, University of Victoria, Victoria V8W 3P6, British Columbia, Canada

³ Subaru Telescope, 650 N. A‘ohoku Place, Hilo, Hawaii 96720, USA

⁴ Institute of Astronomy, University of Cambridge, Madingley Road, Cambridge CB3 0HA, UK

⁵ UK Astronomy Technology Centre, Royal Observatory, Blackford Hill, Edinburgh EH9 3HJ, UK.

Accepted 2000 xxxxxx yy. Received 2000 xxxxxx yy; in original form 2000 xxxxxx yy

ABSTRACT

We present high-precision *JHK* photometry with the 3.8m UK Infrared Telescope (UKIRT) of 83 standard stars, 28 from the widely used preliminary list known as the “UKIRT Faint Standards” (Casali & Hawarden, 1992), referred to here as the Fundamental List, and 55 additional stars referred to as the Extended List. The stars have $9.4 < K < 15.0$ and all or most should be readily observable with imaging array detectors in normal operating modes on telescopes of up to 10m aperture. Many are accessible from the southern hemisphere. Arcsec-accuracy positions (J2000, Epoch ~ 1998) are given, together with optical photometry and spectral types from the literature, where available, or inferred from the $J - K$ colour. K-band finding charts are provided for stars with proper motions exceeding $0.''3 \text{ yr}^{-1}$. We discuss some pitfalls in the construction of flat fields for array imagers and a method to avoid them. On 30 nights between late 1994 and early 1998 the stars from the Fundamental List, which were used as standards for the whole programme, were observed on an average of 10 nights each, and those from the Extended List on an average of 6 nights. The average internal standard error of the mean results for the K magnitudes is $0.^m005$; for the $J - H$ colours it is $0.^m003$ for the Fundamental List stars and $0.^m006$ for those of the Extended List; for $H - K$ the average is $0.^m004$. The results are on the natural system of the IRCAM3 imager, which used a 256×256 InSb detector array with “standard” *JHK* filters, behind gold-coated fore-optics and a gold- or silver-dielectric coated dichroic. We give colour transformations onto the CIT, Arcetri and LCO/Palomar NICMOS systems, and preliminary transformations onto the system defined by the new Mauna Kea Observatory near-infrared filter set.

Key words: infrared: stars - techniques: photometric - stars: general.

1 INTRODUCTION

1.1 Near infrared (NIR) photometric systems

Definition of a near-infrared photometric system was begun by Johnson and colleagues (*c.f.* Johnson 1966 and references therein). The systems which eventually came into widespread use fell into three families (*c.f.* Elias *et al.* 1983). The South African Astronomical Observatory (SAAO) system of Glass (1974) is most recently manifest in the work of Carter (1990) and Carter & Meadows (1995). The AAO

system (Allen & Cragg, 1983) derives from this and more especially from the the Mount Stromlo Observatory (MSO) system (*c.f.* Jones & Hyland, 1982), of which a more recent descendant is the Mount Stromlo and Siding Springs Observatory (MSSSO) system (*c.f.* McGregor, 1994). The Caltech/Tololo (CIT) system was first set out by Frogel *et al.* (1978) and, in a wider sample of fainter stars observed to higher precision, in the defining paper by Elias *et al.* (1982). This has become the default system for NIR photometry in the Northern Hemisphere. Its relation to the Southern Hemisphere systems was explored by Elias *et al.* (1983).

* E-mail: tgh@roe.ac.uk

Local NIR photometric systems have been developed at

the Observatorio Astronómico Nacional, México (Tapia *et al.* 1986, Carrasco *et al.* 1991) and at ESO, where an initial system by Engels *et al.* (1981) was updated by Bouchet *et al.* (1991). Not surprisingly there have been several intercomparisons (*e.g.* Elias *et al.* 1983), sometimes combined with homogenisations (Koorneef 1983a; Bessel & Brett 1988).

Absolute calibrations have been undertaken by several methods. Perhaps the most fundamental approach has been that of the absolute calibration of Vega in the present wavelength range by comparison with a furnace (*e.g.* Blackwell *et al.* 1983). Other approaches have been adopted by, amongst others, Koorneef *et al.*, Bersanelli *et al.* 1991 (who provide a useful summary), Bessel & Brett (1988) and Carrasco *et al.* (1991). More recently Cohen and colleagues have pursued an comprehensive programme (*c.f.* Cohen *et al.* 1999 and references therein) employing a variety of methods, including in particular space-based measurements and the use of model atmospheres to link observed results, to establish a network of bright absolute calibrators over the sky.

1.2 UKIRT “in-house” standards 1980-1992

At the 3.8m UK Infrared Telescope (UKIRT) an in-house (unpublished) set of standard stars, largely drawn from the CIT list, was adopted in the early 1980s. Repeated observations of these stars using the UKIRT single-channel photometer UKT9 and its predecessors were used to accumulate corrections to the catalogue magnitudes and colours for the individual stars. The list therefore established a UKIRT “natural” system, with its K zeropoint based mainly on the early-type stars of the CIT list, and indeed no difference could be discerned between the UKIRT and CIT systems at K (*c.f.* Guianeri, Dixon & Longmore, 1991). The stars became known as the UKIRT Standards, and the list was used extensively through the late 1980s and early 1990s to calibrate measurements with the single-channel “UKT” series of InSb photometers, and also to calibrate spectroscopic observations.

1.3 The need for faint NIR standard stars

Infrared standard stars have traditionally been bright objects, initially, in part, because early detectors were relatively insensitive. The stars comprising the standard lists mentioned in the previous section have K magnitudes between ~ 0 and ~ 8 , with the exception of the list by Carter & Meadows (1995) which includes about 12 objects which are fainter than $K \sim 8.5$ and accessible to Northern telescopes.

Modern near-IR array detectors are enormously more sensitive than the devices used to set up the systems. This sensitivity has been achieved by dramatic reductions in detector read noise, effectively from reductions in detector size: maximum sensitivity is achieved by making the detector capacitance as small as possible, so that signal voltages are maximised relative to the noise of the readout electronics. The signal current is measured by discharging the detector capacitance, and as that capacitance is reduced to increase sensitivity, so the amount of charge that can be measured in the shortest possible integration in normal observing mode (the “well depth”) necessarily also reduces. Unless a non-standard (high-speed) observing mode is employed, such a

system effectively has a fixed dynamic range, and as its sensitivity increases, so the brightest measurable sources become fainter.

This is well illustrated by developments at UKIRT. After 1985 the IRCAM series of instruments (McClean *et al.* 1986) became the “workhorse” imagers. The last of these, IRCAM3 (Puxley *et al.*, 1994) was used from 1991 to 1999 and is the source of all the data presented here. Because of the abovementioned limitations IRCAM3 could not carry out broad-band JHK measurements of stars brighter than $K \sim 9.0$ in normal observing mode, without saturation, unless the telescope was defocussed or the seeing very poor. Such constraints will of course be even more severe for yet larger telescopes.

2 THE UKIRT FAINT STANDARDS

In 1990 a programme was initiated at UKIRT to construct a set of standard stars faint enough to be observable with the IRCAM imager in standard observing mode. A list of stars was selected from Landolt’s (1983) equatorial $UBVRI$ standards and the compilation of potential HST reference sources by Turnshek *et al.* 1990, supplemented by additional main-sequence objects with solar-like colours from the old open cluster M67 (Eggen & Sandage, 1964) and subgiants from the globular clusters M3 and M13, none of which are likely to be variable.

The final list of stars was observed over two years in 1990 and 1991 with the facility single-channel photometer UKT9, using an InSb detector employing charge integration on an external capacitance. The observations were done through apertures of angular diameter $8''$ or $12''$ on the sky, with background removal by chopping with the secondary mirror. The observations were made relative to numerous stars from the CIT-based UKIRT “in-house” standards, mentioned above. The results were made available to users of UKIRT and of other telescopes by Casali & Hawarden (1992), in the UKIRT Newsletter. These stars, the “UKIRT Faint Standards” have been very widely used by observers in the near-IR on large telescopes.

As acknowledged by Casali & Hawarden, the internal precision of their results left something to be desired, especially for the fainter objects. Also, while the majority of the stars have impeccable photometric credentials from Landolt (1983, 1992) some were less well known objects, for which several observations over a number of years were desirable to establish constancy. Other drawbacks, such as the paucity of stars both red enough for transformations and faint enough to observe, and of stars away from the equator, became apparent. Consequently a further programme was initiated in 1994, with the intent of strengthening the mutual precision of the the magnitudes and colours of the UKIRT Faint Standards and simultaneously of supplementing their number with additional stars, widely distributed both in location and in colour. These last comprise the UKIRT Faint Standards Extended List. Not all of the original UKIRT Faint Standards have been retained in this version of the Fundamental List: FS 8,9 and 26 (SA94-251, SA94-702 and SA108-475) were omitted because they were too bright to measure with IRCAM3; FS24 (SA106-1024) is a δ Scuti variable (Landolt, 1990) which exhibits occasional excursions in

the NIR; FS 25 (SA107-1006) and FS 28 (SA109-71) are double, with separations that interfere with photometry using aperture radii of a few arcsec. (FS18 is also double but with a small separation.)

The Extended List standards were selected as follows. An initial selection was made from the Carlsberg Meridian Catalogue (1989), which lists precise positions and good-quality magnitudes, as well as HD spectral types; however few CMC stars proved faint enough in the IR. The majority of the stars in the Extended List were selected from the Guide Star Photometric Catalogue (GSPC, Lasker *et al.* 1988) with a view to reasonably uniform sky coverage and inclusion of a range of colours. These were supplemented by samples of intrinsically red objects (red dwarfs) from Leggett & Hawkins 1988 and Leggett 1992.

Heavily reddened stars behind dark clouds were also sought, and selected stars in B216/217 (Goodman *et al.* 1992), L1641 (Chen *et al.* 1993), Serpens/Ophiuchus (Eiroa & Casali 1992) and Sharpless 106 (Hodapp & Rayner, 1991) were included in the observing list. Intrinsic variability (presumably of young imbedded objects), crowding and problems with bright, structured backgrounds eliminated all the stars in L1641 and S106 and several in Serpens. In the final list four stars from B216 and four from Serpens have been retained.

The B216 objects are designated here by their order in the list of background (“b”) objects in Table 1 of Goodman *et al.* (1992). We note that our K magnitudes agree with the rough NIR results presented by those authors, but our $J-K$ colours are bluer, by up to several tenths of a magnitude; the discrepancies do not correlate with colour.

Nine stars in the final list overlap with Persson *et al.* 1998; differences between our natural system and theirs are discussed in §8.

The positions of the stars were all checked at the telescope. UKIRT observations are made after pointing at a “Nearstar”, usually from the Carlsberg Meridian Catalogue (1989: CMC), which provides positions accurate to $\sim 0.''1$ or better. During this pointing the relationship of the pointing of the telescope guider to the reference point on the array is automatically checked and corrected. After the “Nearstar” pointing the telescope is slewed to the target star, which is typically less than 2° away. When this is completed the telescope pointing gives the position of the star with sub-arcsecond precision relative to the CMC star.

Table 1 lists the Faint Standards, giving our identification number, positions, proper motions (where available from SIMBAD), catalogue designations, spectral types (from the literature when available, or inferred from the $J-K$ colour) and optical photometry. References are given both to the original source from which the star was selected and the sources of the spectral types and photometry. Identification numbers have been assigned to the stars as it has been found that short and unambiguous numbers assist communications in crowded and noisy telescope control rooms. The 28 stars of the Fundamental List have two-digit identification numbers while the 55 stars of the Extended List have three-digit numbers. The positions are accurate to $\sim 1''$ and are expressed in the J2000 co-ordinate system, epoch ~ 1998 . Figure 1 gives K -band finding charts, epoch 2000.8, for the 10 stars with proper motions $\geq 0.''3 \text{ yr}^{-1}$. Optical finding

charts for most of the rest may be found in the source references.

Several of the most obscured and intrinsically reddest stars are difficult or impossible to detect at visible wavelengths, even with large telescopes, and may therefore require to be observed with offset- (or no) guiding.

3 OBSERVATIONS

3.1 The instrument: IRCAM3, its fore-optics and filters.

By 1994 UKIRT was no longer equipped with a photometer, so the array imager IRCAM3 (Puxley *et al.* 1994 and references therein) was employed for all of these observations. As noted above, stars brighter than $K \sim 9.0$ were unobservable with IRCAM3 using the normal readout mode NDSTARE (Chapman *et al.* 1990). At that time there were no standard stars on other systems to which the new observations could be connected which were faint enough to be observable with IRCAM3 in this mode. Consequently the new data are entirely self-referential (*i.e.* calibrated entirely relative to the UKIRT Fundamental List Faint Standards themselves) and are on the natural system of the IRCAM3 imager and its predecessor. However Guarneri *et al.* (1991) showed that this system is close to that of UKT9, the single channel cryostat with which the original observations were made and which had conventionally defined the UKIRT photometric system, and for which transformations to, *e.g.*, the CIT system, are known (Casali & Hawarden, 1992).

IRCAM3 employed an InSb array of 256×256 pixels, each of which subtended an angle of $0.''28$ on the sky. The optical system included three lenses, two of BaF₂ and one of LiF, with total attenuation factor of ~ 0.79 , imperceptibly dependent on wavelength across the range of interest here. It used gold-coated reflecting fore-optics (2 surfaces) and received the infrared beam by reflection from a tertiary mirror carrying a dichroic coating. Until the end of 1996 this was of gold, $\sim 40 \text{ nm}$ thick, with $\sim 25\%$ transmittance for green light, which allowed source acquisition, and guiding, in the optical. The gold coatings (on both dichroic and fore-optics) have proved very stable over the years and no evolution of the UKIRT colour system was ever detected.

The observations were made with the “standard” UKIRT broad-band filters: J ($1.28\mu\text{m}$), H ($1.65\mu\text{m}$), and K ($2.20\mu\text{m}$), transmittance curves for which are specified in Table 2. We also list in the Table the effective transmittance derived by convolving the profiles with a calculated atmospheric transmission for Mauna Kea assuming 1.2 mm of precipitable water. The J and H filters were manufactured by Barr Associates, the K filter by Optical Coating Laboratories Inc. (OCLI).

As part of a programme of telescope enhancements, at the end of 1996 the gold dichroic coating was replaced with a proprietary silver-dielectric (“Ag-di”) multilayer coating with similar reflectivity in the IR but much better transmission at visible wavelengths. Nominal reflectance curves for the gold fore-optics (two reflections) and for the gold and “Ag-di” dichroic coatings are given in Table 3. For the gold coatings these are generic curves, while that for the silver-dielectric dichroic coating is from a witness sample. It has

not been possible to measure the actual dichroics because of the large size of the glass substrates.

Examination of Tables 2 and 3 indicates that the change in the effective wavelength of the *J* filter (the only one likely to be affected by the change from gold to Ag-di dichroic coating) should be well under 1%, so it is not surprising that observations of stars with a wide range of colours made before and after the change in dichroic coating revealed no discernable change in the *J*-band system properties. However changes in *throughput* (zeropoint) with aging of the dichroic coating *have* been observed in the *J* and other bands.

IRCAM3 has now been modified by the addition of internal, cold, magnifying optics, giving a much finer pixel scale and eliminating the warm gold fore-optics. The instrument with which the present observations were carried out is therefore no longer in existence in its original form.

3.2 Observing procedures

The NDSTARE non-destructive “up-the-ramp” array read-out mode (Chapman *et al.* 1990) was employed for all observations in this programme.

The array field-of-view was $\sim 72''$. A series of frames were taken, with the star image located first in the middle of the array and then on a grid of 2 (later 4) other positions, offset by $\pm 8''$ in RA and in DEC. The use of several offset exposures allows correction for the effects of defective pixels.

The resulting images were later combined to build a mosaic, one through each filter, as described in the next section. Exposures varied from 0.5 to 8 seconds between array read-outs (“on-chip” exposure times). When exposures shorter than 5 seconds were employed, several images were coadded in the readout electronics to accumulate at least 5 seconds total exposure before moving to the next array position.

Initially only three images were taken for each mosaic, in order to minimise overheads associated with the crosshead movement and re-acquisition of the images by the autoguider. This proved to have serious drawbacks for the data reduction (see below) so the number of images per mosaic was increased to five and the individual exposure times reduced to give the same total exposure. The observing algorithms (“EXEC”s) were adjusted to give a nominal signal-to-noise ratio ($S/N \geq 100$ for $K < 12$ and ≥ 30 for $K \sim 15$).

As noted above, the observations were carried out using the stars of the Fundamental List as standards. As many as possible of these were observed on each of the 30 nights or part nights devoted to this programme. An average of 10 (minimum 5, maximum 21) Fundamental List stars were observed on each night.

4 IMAGE DATA REDUCTION

Linearity corrections were applied to the raw IRCAM data. Dark frames, of the same duration as the on-chip exposure times employed for the observations, were then subtracted from the images and the result scaled to one second equivalent on-chip exposure time. The images were then normalised to the same average sky signal.

In array photometry “flat-field” frames are required to adjust the sensitivities of the pixels to a uniform value over

the array. This is generally done by taking exposures of a target area on the inside of the dome.

For reasons which are not well understood, satisfactory images for constructing flat-field frames from dome targets have never been successfully secured with imagers at UKIRT. This has necessitated a reliance on images of the sky. A number of exposures, long enough to have a strong background signal on each pixel, are used to determine a flat field frame by median filtering, *i.e.* to form a frame in which the signal in each pixel is the median of the signals in that pixel in the input images.

Because significant instabilities were known to affect the detector array it was believed that flat field corrections should be redetermined at frequent intervals. In the interests of efficiency, the frames secured in the current mosaic were employed. However the use of small numbers of frames leaves the resulting median subject to a potentially important bias, discussed below, and in retrospect it would have been preferable to determine flat-field corrections from occasional sets of deeper and more numerous exposures taken at intervals through each period of observing.

Each image was divided by the appropriate flat-field frame (see below) to remove sensitivity variations.

The final stage of the preparation of the observations for photometric analysis was to combine the three or five reduced frames into a single mosaic frame by adding them together, displaced by the known shifts of the crosshead or telescope, or (optimally) so as to bring the star images on the individual frames into alignment. Since the array has an effective filling factor of 100%, sampling and spatial resolution were not significant issues for the photometry, despite the large pixel size, and the precision of this alignment was not critical.

5 FLAT-FIELD BIAS

5.1 Errors of the median

The median of an odd numbered set of data values is the value at the centre of the distribution of values; for an even numbered set of values it is the mean of the two values closest to the centre. If one element of the data set is in fact not part of the true distribution (*i.e.* is spuriously too low or too high) then ignoring this fact is effectively to use the incorrect algorithm. This will produce a result which is in error by half the difference of the central values of the distribution; the sign of the error will be positive (*i.e.* the result will be too large) if the spurious datum is itself at the high end of the distribution, and negative if the spurious value is low.

In the present context, a pixel with the target star on or near it in a particular frame is *certain* to have a high signal. Clearly the proper data set from which to determine the median *background* level in that pixel should exclude the frame with the star. However, if this frame is retained, the apparent median for the affected pixel(s) will, by the argument above, be spuriously increased by an amount δ equal to half the difference of the signal level values adjacent to the median in that pixel.

5.2 Effects of median errors

In the flat field frame that pixel would therefore be set so as to *reduce* the signal by the corresponding amount in processing an image frame. This is true of all the pixels underlying the particular star image. If the resulting flat field is then used in the reduction of the image which *caused* the problem, the signal level in both the star image and underlying background will be spuriously reduced. The reduction factor for a given pixel with median signal m is therefore

$$R = 1 - \frac{\delta}{m}$$

If there are few (N) frames δ is of the order of the average pixel-to-pixel difference of the background measured on those frames divided by \sqrt{N} .

Flat field bias of this type can be seen in the flat field frame as holes where stars appeared in the input frames (these are all approximately the same depth irrespective of the brightness of the originating star).

The effect of the bias hole will be to reduce the signal from the star *and underlying background* over the whole area of the star image. The brightness of a source is measured by subtraction of a general sky background from the total signal in an aperture surrounding the star. For bright objects, for which the background is negligible, the effect of the flat-field hole will therefore just be a scaling of the source signal by the flat-field bias, i.e. the star will appear too faint by that small fraction. However for fainter objects the background underlying the source image becomes a significant part of the signal from the star aperture; because it is scaled too, the result is a deficit in the total “star” signal relative to the sky level which is subtracted to determine the source flux. Fainter sources will be progressively more seriously underestimated.

5.3 Avoiding flat-field bias

For imaging of *target* objects at known positions on each frame (such as standard stars) the bias is readily eliminated by deriving a separate flat field frame for each image of a mosaic set using only the *other* frames of the set, on which the target is guaranteed to be somewhere other than where it is on the particular frame being reduced.

However this solution meant that the individual early three-frame mosaic observations were reduced using flat fields derived from only two images. The “median” then derived is in fact the mean of the sky signals in each image: and an average of only two frames is drastically affected if a pixel in one frame has some other (non-target) star in it. Under these circumstances an interloping star changes the flat field by half the star’s signal, producing a spectacular hole in the reduced image. In the present programme, if such holes occurred in the measuring aperture all three-frame observations of the field were discarded.

6 PHOTOMETRY

The individual reduced frames were automatically searched for the star image by identifying the brightest pixel in a $20''$ box centred on the expected location in the frame of the image of the star.

Automated aperture photometry was then performed on both the individual reduced images as well as the mosaic image. In all cases a numerical object aperture $8''$ in diameter and a concentric sky annulus with inner diameter $12''$ and outer diameter $16''$ were used. The median signal in the sky annulus (effectively immune to the bias discussed above from the inclusion of stars or holes, because values from hundreds of pixels were involved in its derivation) was taken as the sky signal per pixel to be subtracted from the object counts to get the true star signal, which was converted to an instrumental magnitude in the usual way.

For the stars of the Fundamental List the instrumental magnitude and the current catalogue magnitude were added to produce a zeropoint magnitude (conventionally the magnitude of a source giving one data number per second through the telescope and photometer system).

6.1 Identifying faulty images

During the initial extraction of the photometric data the images were displayed one by one as they were analysed. This allowed poor images to be noted and possibly discarded. During the subsequent data analysis the standard deviation (σ) of the zeropoints of the individual images of the mosaic were calculated. If this standard deviation exceeded $0.^m1$ then that image was flagged and re-checked visually. If the auto-selection for that image was incorrect, then the star was selected manually. If the image was found to be too distorted to measure (*e.g.* because of bad tracking) it was discarded. If on visual inspection no problems were evident the photometry of the flagged images was retained in the data set.

6.2 Atmospheric extinction and system zeropoints

The zeropoints from each mosaic were differenced to form raw $J - H$ and $H - K$ colours as well as K magnitudes, which were plotted against airmass to derive extinctions. Reductions were performed using the colours rather than the magnitudes in order to preserve the small but significant gain in precision that arises when different wavelengths are observed consecutively in time with minimum change to the instrument, *i.e.* when the *differential changes* are minimised.

Linear fits to the plots against airmass were used to determine extinction coefficients and overall (zenith) zeropoints in each magnitude and colour for each night. The measurements were reduced to the zenith, not to outside the atmosphere, to preserve their internal precision. Absolute precision is much harder to achieve because of strong non-linearity of extinction curves between 1.0 and zero airmass arising from the presence of saturated absorption features (Forbes, 1848; for more accessible references and discussion see Young, Milone & Stagg, 1994). The extinction curves between 2.0 and 1.0 airmass are also in fact non-linear, but the departure from linearity is expected to be unimportant for reductions to the zenith (*c.f.* Young *et al.* 1994).

The data were filtered using the dispersions of the individual frames about the mosaic mean: magnitudes or colours with quadratically combined errors $\sigma > 0.^m1$, were omitted from the analysis. The zeropoints and extinction coefficients were in turn used to reduce the measurements of the stars

on the Extended List. For the stars of the Fundamental List the residuals of all measurements from the extinction curves were ledgered.

6.3 Iterative error trapping

The results for each star on each night were tabulated and overall means and standard deviations σ of $J - H$, $H - K$, and K determined.

An iterative error trapping process was then applied: the measurement with the largest residual in each set of results was identified and new means and σ s calculated with that measurement omitted; if thereafter its residual was more than 3σ from the new mean, the images used in producing the flagged results were once again re-examined for problems (stars or “holes” in the measuring aperture; poor images): if any were found the observation was re-reduced without the offending frame(s), or rejected.

The nightly extinction curves and zeropoints were then redetermined using the new results. The re-reduced colours and magnitudes were once again tabulated and the above procedure repeated until the images associated with all flagged residuals were double-checked and found to be satisfactory.

A final error trapping iteration was then carried out on the finished data table, using the same 3σ criterion as before. This time a decision was taken whether to include or exclude a measurement from the final data set, based for example on the now well-known “typical” error of an observation: *e.g.* measurements differing from the mean by more than 3σ , simply because that particular data set had an atypically small dispersion, were identified and retained.

7 RESULTS

Table 4 gives FS (Faint Standard) numbers, positions, the mean K magnitudes, $J - H$ and $H - K$ colours and the standard errors of these means (SEM), together with the number of nights (N) of observations contributing to the final results. Note that since the stars of the Fundamental List were the reference stars for the total observing list, these stars were generally observed several times more often than the Extended List stars. For the Fundamental List the mean SEM is $0.^m0045$ for K , $0.^m0034$ for $J - H$ and $0.^m0040$ for $H - K$, and the stars were observed between 10 and 31 times on an average of 10 nights. Each star of the Extended List was observed once or (occasionally) twice on each of an average of 6 nights. The average internal standard error of the mean results are $0.^m005$ for the K magnitudes, $0.^m006$ for the $J - H$, and $0.^m004$ for the $H - K$ colours. (The larger average $J - H$ residual for the Extended List arises from the inclusion of very red objects which are markedly fainter at J .)

8 COMPARISONS WITH OTHER SYSTEMS

8.1 The CIT system

Casali & Hawarden (1992) list transformations from the UKT9 natural system at UKIRT to the CIT system:

$$\begin{aligned} K_{CIT} &= K_{UKIRT} - 0.018(J - K)_{UKIRT} \\ (J - K)_{CIT} &= 0.936(J - K)_{UKIRT} \\ (H - K)_{CIT} &= 0.960(H - K)_{UKIRT} \\ (J - H)_{CIT} &= 0.920(J - H)_{UKIRT} \end{aligned}$$

As noted above Guarnieri *et al.* 1991 found that differences between UKT9 and IRCAM photometry at UKIRT must be less than 2% for stars with $J - K < 1$ and so the above transformations are valid for converting the results presented here to the CIT system.

8.2 LCO/Palomar NICMOS

Persson *et al.* (1998) present JHK and Ks results for 65 solar-type stars with $10.^m4 < K < 12.^m2$, covering both hemisphere of the sky, together with 27 redder objects to assist in determining system transformations. The internal precision appears to be slightly poorer than the current results.

The UKIRT Extended List contains 9 stars in common with Persson *et al.*. Eight of these (P525-E, P533-D, P161-D, P212-C, P266-C, S867-V, P565-C and S893-D) are solar-type and one (LHS2397a) is a red dwarf, found to be slightly variable at I by Martin, Zapatero-Osorio & Rebolo (1996). There are no obvious colour terms seen in this limited comparison sample but there does seem to be a constant zero-point difference such that (removing 1-2 outliers for each mean and standard deviation):

$$\begin{aligned} J_{NICMOS} - J_{UKIRT} &= 0.034 \pm 0.004 \\ H_{NICMOS} - H_{UKIRT} &= 0.027 \pm 0.007 \\ K_{NICMOS} - K_{UKIRT} &= 0.015 \pm 0.007 \end{aligned}$$

8.3 Arcetri/ARNICA system

Hunt *et al.* (1998) observed fields around the northern 22 of the original UKIRT Faint Standards, as well as 15 A0 stars selected from the SAO catalogue and 3 deep CCD fields. These 40 fields contain 86 stars measured on between 3 and 10 nights and which have $7.^m9 < K < 14.^m5$. These data are also calibrated relative to the UKIRT Faint Standards. Their internal precision appears to be similar to that of the present results except for the fainter objects: the two data sets agree within their combined errors except for the 4 stars with $K > 13.5$, which are all discrepant by 2σ or more.

8.4 Mauna Kea Observatory near-infrared (MKO-NIR) system

Both UKIRT cameras (the UKIRT Fast Track Imager, UFTI, and the modified IRCAM) are now equipped with filters from the Mauna Kea Consortium (the Mauna Kea Observatory Near-IR (MKO-NIR) filter set: see Simons & Tokunaga, 2001 and Tokunaga & Simons 2001).

These filters have been designed for maximum throughput and minimum background (and therefore maximum sensitivity) at the same time as having a much better match to the atmospheric windows than their precursors. This last implies minimal sensitivity of the results to atmospheric water vapour (the absorption spectrum of which defines most

of the natural NIR atmospheric windows). Because this excludes most of the saturated absorption features which give rise to the Forbes Effect (c.f. Young *et al.*, 1994, and references therein) the extinction curves for these filters are expected to show little or no non-linearity, even between 1.0 and zero airmass. Comparison of results between sites (and nights) with differing water vapour columns should be greatly facilitated thereby, as will the determination of extra-atmospheric (absolute) fluxes. The filters are also of excellent optical quality.

The MKO-NIR system has been endorsed by the IAU Working Group on Infrared Photometry as the preferred standard photometric system for the near infrared.

An MKO-NIR filter set has been in UFTI since commissioning in October 1998, and replaced the old *JHK* set in IRCAM prior to commissioning of its new plate scale in September 1999. Both the *J* and *H* filters are significantly different from the old filters and hence the magnitudes for the Faint Standards on the old IRCAM3 system are no longer on the natural systems of the imagers. Colour transformations have been derived in two ways: one empirically based on UFTI photometry and the other calculated by convolving the known filter profiles with spectroscopic data for a representative set of red stars. The two determinations agree well. Note that the transformations for IRCAM after its modifications should be identical with those for UFTI, since its optics have flat transmission curves across the *J*, *H* and *K* windows and both array response curves are also flat across this wavelength range.

The transformations between the old IRCAM3 system and the new MKO-NIR system at *H* and *K* are well behaved and single-valued. However for the *J* filter different terms have to be applied depending on whether or not the standard star has intrinsic water absorption features. This is due to the fact that the MKO-NIR *J* filter cuts off at a shorter wavelength than the old filter, specifically to avoid water absorption in the terrestrial atmosphere. We have determined that for stars with no intrinsic water features the colour transformations between the MKO-NIR system and the system of the results presented here are:

$$\begin{aligned} K_{UKIRT} &= K_{MKO} + 0.020[+/- 0.005](J - K)_{MKO} \\ (J - H)_{UKIRT} &= 1.040[+/- 0.010](J - H)_{MKO} \\ (H - K)_{UKIRT} &= 0.830[+/- 0.010](H - K)_{MKO} \\ (J - K)_{UKIRT} &= 0.960[+/- 0.010](J - K)_{MKO} \end{aligned}$$

or:

$$\begin{aligned} K_{MKO} &= K_{UKIRT} - 0.020[+/- 0.005](J - K)_{UKIRT} \\ (J - H)_{MKO} &= 0.960[+/- 0.010](J - H)_{UKIRT} \\ (H - K)_{MKO} &= 1.205[+/- 0.010](H - K)_{UKIRT} \\ (J - K)_{MKO} &= 1.040[+/- 0.010](J - K)_{UKIRT} \end{aligned}$$

However for stars with significant water absorption, *i.e.* stars of spectral types M4 through late L (but not including the T class with methane absorption):

$$\begin{aligned} K_{MKO} &= K - 0.020[+/- 0.005](J - K)_{UKIRT} \\ (J - H)_{MKO} &= 0.870[+/- 0.010](J - H)_{UKIRT} \\ (H - K)_{MKO} &= 1.205[+/- 0.010](H - K)_{UKIRT} \\ (J - K)_{MKO} &= 0.980[+/- 0.010](J - K)_{UKIRT} \end{aligned}$$

We expect soon to re-observe all the UKIRT Faint Standards, and all accessible LCO/Palomar NICMOS standards, using the new filter set, in order to place these stars accurately onto the MKO-NIR system.

Acknowledgments

This programme was made possible by the use of “continuity” engineering time during the UKIRT Upgrades Programme, 1993-1998 (c.f. Hawarden *et al.* 1999). We are therefore especially grateful to Dr. Tom Geballe, then Head of UKIRT Operations, for assisting us to exploit this opportunity. Many of our other colleagues at UKIRT provided extensive advice, assistance and support. We are grateful to Prof. Marcia Rieke for providing us with a preliminary list of the NICMOS stars which enabled us to incorporate a subset in the present programme.

REFERENCES

- Allen, D.A. & Cragg, T.A., 1983. MNRAS, 203, 777
- Bersanelli, M., Bouchet, P. & Falomo, R., 1991. A & A, 252, 854
- Bessell, M.S. & Brett, J.M., 1988. PASP, 100, 1134
- Blackwell, D.E., Leggett, S.K., Petford, A.D., Mountain, C.M. & Selby, M.J., 1983. MNRAS, 205, 897.
- Bouchet, P., Manfroid, J. & Schmider, F.X., 1991. A & A Supp., 91, 409
- Carrasco, L., Recillas-Cruz, E., Garcia-Barreto, A., Cruz-Gonzalez, I. & Serrano, A.P.G., 1991. PASP, 103, 987
- Carter, B.S., 1990. MNRAS, 242, 1
- Carter, B.S. & Meadows, V.S., 1995. MNRAS, 276, 734
- Casali, M.M. & Hawarden, T.G., 1992. The JCMT-UKIRT Newsletter, 4, 35
- Carlsberg Meridian Catalogue La Palma, No 4, 1989. Copenhagen University observatory, Royal Greenwich Observatory & Real Instituto y Observatorio de la Armada en San Fernando (Servicio Publicaciones Armada).
- Chapman, R., Beard, S.M., Mountain, C.M., Pettie, D.G., Pickup, D.A. & Wade, R., 1990. Proc. SPIE, 1235, 34
- Chen, H., Tokunaga, A.T., Strom, K.M. & Hodapp, K.-W., 1993. ApJ, 407, 639
- Chevalier, C. & Ilovaisky, S.A., 1991. A & A Suppl., 90, 225
- Cohen, M., Walker, R.G., Carter, B., Hammersley, P.L., Kidger, M.R. & Noguchi, K., 1999. AJ, 117, 1864
- Drilling, J.S. & Landolt, A.U., 1979. ApJ, 84, 783
- Eggen, O.J. & Sandage, A.R., 1964. ApJ, 140, 130
- Elias, J.H. Frogel, J.A., Matthews, K & Neugebauer, G., 1982. AJ, 87, 1029
- Elias, J.H., Frogel, J.A., Hyland, A.R. & Jones, T.J., 1983. AJ, 88, 1027
- Eiroa, C. & Casali, M.M., 1992. A&A 262, 468
- Forbes, J.D., 1848. Phil. Trans., 132, 225
- Frogel, J.A., Persson, S.E., Aaronson, M. & Matthews, K., 1978. ApJ, 220, 75
- Glass, I. S., 1974. Mon Notes Astr. Soc. S. Africa, 33, 53
- Goodman, A.A., Jones, T.J., Lada, E.A. & Myers, P.C., 1992. ApJ, 399, 108
- Greenstein, J.L., 1966. ApJ, 144, 496
- Guarnieri, M.D., Dixon, R.I. & Longmore, A.J., 1991. PASP, 103, 675
- Hawarden, T.G., Rees, N.P., Chuter, T.C., Chrysostomou, A.C., Cavedoni, C.P., Rohloff, R.-R., Pitz, E., Pettie, D.G., Bennett, R.J. & Atad-Ettdgui, E., 1999. Proc SPIE, 3785, 82

- Hodapp, K.-W. & Rayner, J., 1991. AJ, 102, 1108
 Hunt, L.K., Mannucci, F., Testi, L., Migliorini, S., Stanga, R.M.,
 Baffa, C., Lisi, F. & Vanzi, L., 1998. AJ, 115, 2594
 Johnson, H.L., 1996. Ann. Rev. Astron. Astrophys., 3, 193
 Klemola, A.R., 1962. AJ, 67, 740
 Koorneef, J., 1983a. A & A, 128, 84
 Koorneef, J., 1983b. A & A Suppl., 51, 489
 Landolt, A.U., 1983. AJ, 88, 439
 Landolt, A.U., 1990. PASP, 102, 1382
 Landolt, A.U., 1992. AJ, 104, 340
 Lasker, B.M., Sturch, C.R., Lopez, C., Mallama, A.D., McLaughlin, S.F., Russell, J.F., Wisniewski, W.Z., Gillespie, B.A., Jenkner, H., Siciliano, E.D., Kenny, D., Baumert, J.H., Goldberg, A.M., Henry, G.W., Kemper, E. & Siegel, M.J., 1988. Ap.J. Supp, 68, 1
 Leggett, S.K. 1992. Ap.J. Supp., 82, 351
 Leggett, S.K., Harris, H.C. & Dahn, C., 1994. AJ 108, 944
 Leggett, S.K. & Hawkins, M.R.S., 1988. MNRAS 234, 1065
 Luyten, W.J., 1979, LHS Catalogue Minneapolis: University of Minnesota
 Martin, E.L., Zapatero-Osorio, M.R., & Rebolo, R., 1996. 9th Cambridge workshop on "Cool stars, stellar systems & the sun", eds. R.Pallavicini & A.Dupree, ASP Conf. Series 109, 615
 McClean, I.S., Chuter, T.C., McCaugrean, M.J. & Rayner, J.T., 1986. Proc. SPIE, 637, 430
 McCook, G.P., & Sion, E.M., 1987. ApJS, 65, 603
 McGregor, P.J., 1994. PASP, 106, 508
 Persson, S.E., Murphy, D.C., Krzeminiski, W., Roth, M. & Rieke, M.J., 1998. AJ, 116, 2475
 Pesch, P., 1967. ApJ, 148, 781
 Puxley, P.J., Sylvester, J, Pickup, D.A., Paterson, M.J., Laird, D.C. & Atad-Ettdgui, E, 1994. Proc. SPIE, 2198, 350
 Sandage, A.R. & Katem, B., 1982. AJ, 87, 537
 Simons, D. & Tokunaga, A., 2001. PASP submitted
 Straizys, V. & Kalytis, R., 1981. Act. Astron., 31, 93
 Tapia, M., Neri, L. & Roth, M., 1986. Rev. Mex. Astron. Astrof., 13, 115
 Tokunaga, A. & Simons, D., 2001. PASP submitted
 Turnshek, D.A., Bohlin, R.L., Williamson, R.L. II, Lupie, O.L., Koorneef, J. & Morgan, D.H., 1990. AJ, 99, 1243
 Young, A.T., Milone, E.F. & Stagg, C.P., 1994. A & A Suppl., 105, 259

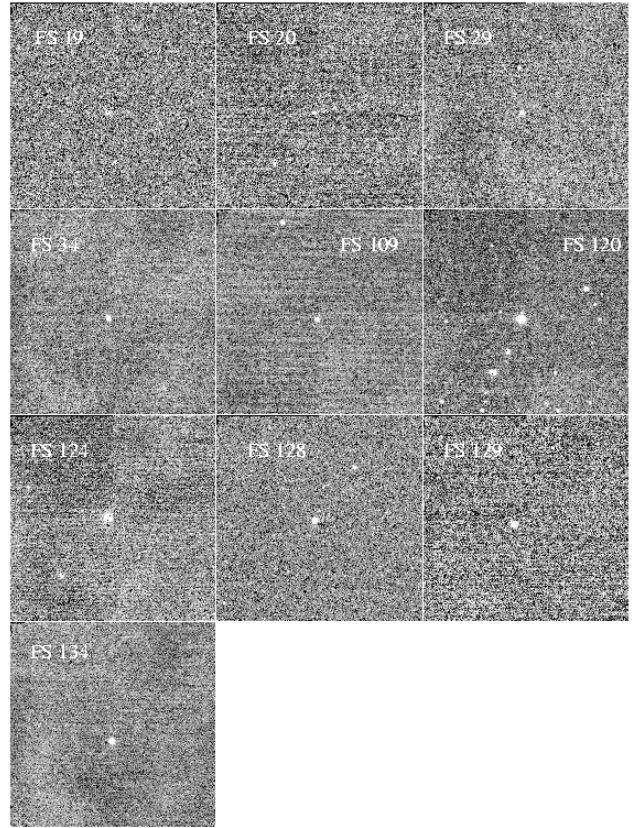


Figure 1. Finding charts (epoch 2000.8) for the UKIRT Faint Standards with proper motions larger than $0.''3 \text{ yr}^{-1}$. The images were taken through a K filter. Each is $93''$ square; North is up, East to the left.

Table 1. The UKIRT Faint Standards: names, spectral types, optical photometry and references.

FS	RA (J2000)	Dec	PM-RA " yr ⁻¹	PM-Dec " yr ⁻¹	Other Name	Source Ref.	Spectral Type	Spec. Ref.	V	B − V	V − I	Phot. Ref.
101	00 13 43.58	+30 37 59.9	−0.005	−0.009	CMC 400101	11	F0	21	11.7:	0.0:	-	11
102	00 24 28.50	+07 49 00.1	-	-	P525-E	12	G3	*	13.90	1.17	-	12
1	00 33 54.48	−12 07 58.1	0.152	−0.179	G158-100	2	DK-G	2	14.89	0.69	-	2
103	00 36 29.60	+37 42 54.3	-	-	P241-G	12	K2	*	14.32	1.05	-	12
2	00 55 09.93	+00 43 13.1	-	-	SA92-342	1	F5	5	11.61	0.44	0.54	9
3	01 04 21.63	+04 13 36.0	-	-	Feige 11	1,2	sdB	6	12.06	−0.24	−0.26	9
104	01 04 59.43	+41 06 30.8	0.000	−0.004	P194-R	12	A7	*	11.03	0.18	-	12
105	01 19 08.19	+07 34 11.5	-	-	P527-F	12	K1	*	13.43	1.03	-	12
106	01 49 46.94	+48 37 53.2	-	-	P152-F	12	K4	*	14.77	1.31	-	12
107	01 54 10.14	+45 50 38.0	−0.025	−0.004	CMC 600954	11	G0	21	11.3:	0.7:	-	11
5	01 54 34.65	−06 46 00.4	-	-	Feige 16	1,2	A0	6	12.41	−0.01	−0.00	9
4	01 54 37.70	+00 43 00.5	-	-	SA93-317	1	F5	5	11.55	0.49	0.59	9
6	02 30 16.64	+05 15 51.1	0.071	−0.025	Feige 22	1,2	DA3	8	12.80	−0.05	−0.21	9
7	02 57 21.21	+00 18 38.2	-	-	SA94-242	1	A2	5	11.73	0.30	0.36	9
108	03 01 09.85	+46 58 47.7	0.001	−0.001	CMC 502032	11	F8	21	11.2:	0.4:	-	11
109	03 13 24.16	+18 49 38.4	1.246	−1.087	LHS 169	13	M2V	14	14.13	1.45	1.72	14
110	03 41 02.22	+06 56 15.9	-	-	P533-D	12	G5	*	13.20	0.70	-	12
111	03 41 08.55	+33 09 35.5	0.003	0.003	CMC 601790	11	G5	21	11.3:	0.9:	-	11
112	03 47 40.70	−15 13 14.4	-	-	S618-D	12	G0	*	12.30	0.55	-	12
10	03 48 50.20	−00 58 31.2	-	-	GD50	2	DA2	8	13.99	−0.21	-	8
113	04 00 14.07	+53 10 38.5	-	-	P117-F	12	K0	*	14.90	1.03	-	12
114	04 19 41.72	+16 45 22.4	-	-	Hy214	15	M7V	15	21.05	-	4.17	16
115	04 23 18.17	+26 41 16.4	-	-	B216-b5	18	-	-	-	-	-	-
116	04 23 50.18	+26 40 07.7	-	-	B216-b7	18	-	-	-	-	-	-
117	04 23 56.61	+26 36 38.0	-	-	B216-b9	18	-	-	-	-	-	-
118	04 24 33.49	+26 33 37.8	-	-	B216-b13	18	-	-	-	-	-	-
11	04 52 58.92	−00 14 41.6	-	-	SA96-83	1	A3	5	11.72	0.18	0.19	9
119	05 02 57.44	−01 46 42.6	0.001	−0.006	SAO 131719	11	A2	21	10.14	0.10	-	11
12	05 52 27.66	+15 53 14.3	0.096	−0.189	GD71	1	sdO	8	13.03	−0.25	0.30	9
13	05 57 07.59	+00 01 11.4	-	-	SA97-249	1	G4V	5	11.74	0.65	0.72	9
120	06 14 01.44	+15 09 58.3	0.751	−1.220	LHS 216	13	M1V	14	14.66	1.62	2.08	14
121	06 59 46.82	−04 54 33.2	-	-	S772-G	12	K3	*	14.21	1.20	-	12
122	07 00 52.02	+48 29 24.0	-	-	P161-D	12	G0	*	12.85	0.57	-	12
14	07 24 14.40	−00 33 04.1	-	-	Rubin 149	2	O9-B2p	2	13.86	−0.14	-	2
15	08 51 05.81	+11 43 46.9	-	-	M67-I-48	3	G5IV-V	*	14.05	0.70	-	3
123	08 51 11.88	+11 45 21.5	−0.008	−0.006	P486-R (Note 4)	12	B8V	19	10.02	−0.08	−0.07	20
16	08 51 15.01	+11 49 21.2	-	-	M67-IV-8	3	G1V	*	14.18	0.61	-	3
17	08 51 19.31	+11 52 10.4	-	-	M67-IV-27	3	G4V	*	13.95	0.61	-	3
18	08 53 35.51	−00 36 41.7	-	-	SA100-280	1	F8	5	11.80	0.49	0.59	9
124	08 54 12.07	−08 04 58.9	0.939	−0.810	LHS 254	13	M5V	14	17.41	1.75	3.97	14
125	09 03 20.60	+34 21 03.9	-	-	P259-C	12	G8	*	12.11	0.67	-	12
126	09 19 18.73	+10 55 54.2	-	-	P487-F	12	K3	*	14.48	1.03	-	12
127	10 06 29.03	+41 01 26.6	-	-	P212-C	12	F9	*	13.03	0.52	-	12
19	10 33 42.75	−11 41 38.3	−0.297	−0.055	G162-66	1,2	DA2	8	13.01	−0.16	−0.27	9
128	11 05 10.40	+07 06 48.7	−0.508	−0.156	LHS 2347	13	M5V	14	19.00	-	−3.88	14
20	11 07 59.93	−05 09 26.1	−0.038	−0.426	G163-50	1,2	DA3	8	13.06	0.04	−0.16	9
129	11 21 48.95	−13 13 07.9	−0.400	−0.349	LHS 2397a	13 (Note 1)	M8V	14	19.57	-	4.62	14
130	11 24 55.92	+34 44 38.5	-	-	P264-F	12	K4	*	15.07	1.40	-	12
21	11 37 05.15	+29 47 58.4	−0.147	−0.006	GD140	4	DA3	8	12.50	−0.06	-	8
131	12 14 25.40	+35 35 55.6	-	-	P266-C	12	F8	*	12.56	0.51	-	12

Table 1 – *continued*

FS	RA (J2000)	Dec	PM-RA " yr ⁻¹	PM-Dec " yr ⁻¹	Other Name	Source Ref.	Spectral Type	Sp. Ref.	V	B – V	V – I	Phot. Ref.
132	12 21 39.36	–00 07 13.3	-	-	S860-D	12	G1	*	13.33	0.55	-	12
33	12 57 02.30	+22 01 52.8	0.007	–0.198	GD153	4	DA1	8	13.42	–0.25	-	8
133	13 15 52.80	+46 06 36.9	-	-	P172-E	12	G9	*	13.73	0.69	-	12
23	13 41 43.57	+28 29 49.5	-	-	M3-VZ193	4	G8III	*	14.75	0.90	-	10
134	14 28 43.37	+33 10 41.5	–0.354	–0.720	LHS 2924	13 (Note 1)	M9V	14	19.58	-	4.37	14
135	14 40 58.04	–00 27 46.6	-	-	S867-V	12	G5	*	13.34	0.68	-	12
136	14 59 32.05	–00 06 17.0	-	-	S868-G	12	K2	*	14.68	1.12	-	12
137	16 26 42.72	+05 52 20.3	-	-	P565-C	12	G1	*	13.34	0.54	-	12
138	16 28 06.72	+34 58 48.3	–0.012	0.005	P275-A	12	A1	*	10.45	0.00	-	12
139	16 33 52.96	+54 28 22.1	-	-	P137-F	12	K1	*	14.61	1.05	-	12
27	16 40 41.56	+36 21 12.4	-	-	-	Note 2	G8IV/V	*	14.8:	0.7:	-	-
140	17 13 22.65	–18 53 33.8	-	-	S587-T	12	G9	*	12.29	0.72	-	12
141	17 48 58.87	+23 17 43.7	-	-	P389-D	12	G2	*	12.51	0.78	-	12
35	18 27 13.52	+04 03 09.4	-	-	-	Note 3	K0	*	10.0:	0.8:	-	-
142	18 29 51.26	+01 13 19.0	-	-	Ser-EC51	17	-	-	-	-	-	-
143	18 29 53.79	+01 13 29.9	-	-	Ser-EC68	17	-	-	-	-	-	-
144	18 29 56.90	+01 12 47.1	-	-	Ser-EC84	17	-	-	-	-	-	-
145	18 30 05.81	+01 13 47.3	-	-	Ser-EC160	17	-	-	-	-	-	-
146	18 54 04.01	+37 07 18.6	-	-	P280-U	12	K1	*	12.67	0.99	-	12
147	19 01 55.27	+42 29 19.6	–0.001	0.000	P230-A (Note 4)	12	A0	21	10.02	0.07	-	12
148	19 41 23.41	–03 50 56.9	–0.001	–0.004	S810-A (Note 4)	12	A0	21	9.69	–0.07	-	12
149	20 00 39.25	+29 58 40.0	0.005	–0.004	P338-C (Note 4)	12	B7.5V	22	10.41	0.01	-	22
150	20 36 08.44	+49 38 23.5	0.008	0.009	CMC 513807	21	G0	21	10.9:	0.4	-	11
34	20 42 34.73	–20 04 34.8	0.355	–0.098	EG141	4	DA3	8	12.34	–0.07	-	8
151	21 04 14.75	+30 30 21.2	-	-	P340-H	12	G2	*	13.53	0.68	-	12
29	21 52 25.36	+02 23 20.7	0.023	–0.303	G93-48	1,2	DA3	8	12.74	–0.01	–0.19	9
152	22 27 16.12	+19 16 59.2	-	-	p460-E	12	K1	*	13.57	1.03	-	12
30	22 41 44.72	+01 12 36.5	-	-	SA114-750	1	B9	5	11.92	–0.04	0.12	9
153	23 02 32.07	–03 58 53.1	0.018	0.000	S820-E	12	K2		13.96	1.21	-	12
31	23 12 21.60	+10 47 04.1	0.130	–0.011	GD246	1,2	DA1	8	13.09	–0.32	–0.33	9
32	23 16 12.37	–01 50 34.6	-	-	Feige 108	1,2	DAs	7	12.96	–0.24	–0.24	9
154	23 18 10.08	+00 32 55.6	-	-	S893-D	12	G0	*	12.53	0.65	-	12
155	23 49 47.82	+34 13 05.1	-	-	CMC 516589	11	K5	21	12.1:	-	-	11

* MK spectral type estimated from $J - K$ colours (*via* Koornneef 1983a, assuming luminosity class V) or position in cluster CMD, where known.

References in Table 1.

1. Landolt, 1983; 2. Turnshek *et al.* 1990; 3. Eggen & Sandage, 1964; 4. B. Zuckerman, 1990 personal communication; 5. Drilling & Landolt, 1979; 6. Klemola, 1962; 7. Greenstein, 1966; 8. McCook & Sion, 1987; 9. Landolt, 1992; 10. Sandage & Katem 1982; 11. Carlsberg Meridian Catalogue 1989; 12. Lasker *et al.* 1988; 13. Luyten 1979; 14. Leggett 1992; 15. Leggett & Hawkins 1988; 16. Leggett *et al.* 1994; 17. Eiroa & Casali 1992; 18. Goodman *et al.* 1992; 19. Pesch 1967; 20. Chevalier & Ilovaisky, 1991; 21. Henry Draper catalog; 22. Straizys & Kalytis, 1981.

Notes:

(1) FS 129 (= LHS 2397a) and FS 134 (= LHS 2924) are listed by Martin *et al* (1996) amongst very cool dwarfs showing semi-regular variability (probably from surface features and rotation), with respective ranges at I of 0.^m08 and 0.^m06. These are considerably larger than the ranges seen during the present observations, especially of LHS 2924 (see Table 4).

(2) FS 27 is 13.5 from M13; its colour and magnitude are consistent with it being an outlying subgiant member of the cluster. Its optical magnitude and colour are inferred from the IR.

(3) FS 35 was intended to be G21-15, but the coordinates used (from Turnshek *et al.* 1990) were incorrect. (Those in Landolt 1983 & 1992 are correct, however.) This was not noticed until an anonymous star close to the erroneous coordinates had been well observed and has accordingly been retained here; 29 *JHK* observations on 15 nights show no obvious signs of variability. Its optical magnitude and colour are inferred from the IR.

(4) FS 123 = P486-R = M67-F81; FS 147 = P230A = SAO 48018; FS 148 = S810-A = HD 185879; FS 149 = P338-C = HD 333240.

Table 2. Transmission curves of UKIRT (IRCAM) *JHK* filters at 77K, with and without atmospheric transmission effects of a 1.2mm H₂O column.

<i>J</i>			<i>H</i>			<i>K</i>		
λ μm	Trans. %	with atm.%	λ μm	Trans. %	with atm. %	λ μm	Trans. %	with atm. %
1.05	0.000	0.000	1.42	0.002	0.001	1.86	0.000	0.000
1.06	0.000	0.000	1.43	0.000	0.000	1.88	0.002	0.000
1.07	0.011	0.011	1.44	0.001	0.001	1.90	0.005	0.001
1.08	0.015	0.015	1.45	0.005	0.004	1.92	0.016	0.006
1.09	0.028	0.028	1.46	0.009	0.008	1.94	0.059	0.037
1.10	0.045	0.044	1.47	0.012	0.009	1.96	0.152	0.107
1.11	0.088	0.085	1.48	0.022	0.018	1.98	0.276	0.253
1.12	0.174	0.139	1.49	0.039	0.037	2.00	0.420	0.265
1.13	0.334	0.283	1.50	0.059	0.060	2.02	0.552	0.405
1.14	0.511	0.464	1.51	0.100	0.098	2.04	0.622	0.599
1.15	0.608	0.529	1.52	0.176	0.175	2.06	0.636	0.556
1.16	0.661	0.634	1.53	0.298	0.298	2.08	0.651	0.641
1.17	0.705	0.698	1.54	0.476	0.474	2.10	0.682	0.675
1.18	0.745	0.736	1.55	0.630	0.630	2.12	0.713	0.708
1.19	0.759	0.751	1.56	0.713	0.713	2.14	0.723	0.723
1.20	0.743	0.735	1.57	0.750	0.735	2.16	0.707	0.705
1.21	0.727	0.720	1.58	0.766	0.749	2.18	0.686	0.685
1.22	0.743	0.739	1.59	0.780	0.780	2.20	0.683	0.680
1.23	0.765	0.765	1.60	0.811	0.797	2.22	0.702	0.702
1.24	0.787	0.787	1.61	0.830	0.809	2.24	0.737	0.737
1.25	0.784	0.784	1.62	0.842	0.842	2.26	0.771	0.767
1.26	0.776	0.768	1.63	0.838	0.838	2.28	0.777	0.776
1.27	0.768	0.733	1.64	0.832	0.829	2.30	0.754	0.754
1.28	0.770	0.767	1.65	0.830	0.825	2.32	0.737	0.735
1.29	0.795	0.792	1.66	0.830	0.829	2.34	0.739	0.732
1.30	0.809	0.800	1.67	0.821	0.821	2.36	0.733	0.710
1.31	0.804	0.775	1.68	0.831	0.830	2.38	0.654	0.641
1.32	0.802	0.750	1.69	0.844	0.842	2.40	0.470	0.458
1.33	0.805	0.722	1.70	0.843	0.842	2.42	0.268	0.243
1.34	0.818	0.741	1.71	0.848	0.846	2.44	0.128	0.128
1.35	0.832	0.568	1.72	0.851	0.848	2.46	0.055	0.054
1.36	0.829	0.222	1.73	0.850	0.847	2.48	0.023	0.019
1.37	0.818	0.265	1.74	0.849	0.839	2.50	0.010	0.009
1.38	0.811	0.294	1.75	0.838	0.832	2.52	0.004	0.003
1.39	0.813	0.498	1.76	0.846	0.838	2.54	0.001	0.000
1.40	0.768	0.290	1.77	0.838	0.821	2.56	0.000	0.000
1.41	0.602	0.334	1.78	0.826	0.786			
1.42	0.320	0.199	1.79	0.774	0.737			
1.43	0.124	0.095	1.80	0.629	0.483			
1.44	0.054	0.041	1.81	0.413	0.309			
1.45	0.022	0.016	1.82	0.206	0.099			
1.46	0.014	0.012	1.83	0.097	0.040			
1.47	0.001	0.001	1.84	0.053	0.014			
1.48	0.002	0.002	1.85	0.022	0.008			
1.49	0.001	0.001	1.86	0.009	0.002			
1.50	0.000	0.000	1.87	0.001	0.000			
			1.88	0.000	0.001			

Table 3. Reflectance curves of fore-optics of the IRCAM3 imager.

$\lambda(\mu\text{m})$	Gold x 2 (generic)	Gold Dichroic ~40 nm thick	Zeiss “Ag-di” dichroic
0.7	0.921	0.876	-
0.8	0.948	0.906	0.720
0.9	0.956	0.927	0.825
1.0	0.964	0.940	0.883
1.5	0.966	0.952	0.952
2.0	0.970	0.970	0.960
2.5	0.970	0.972	0.970

Table 4. Positions, K magnitudes and JHK colours and their uncertainties, and the number of nights observed, for the UKIRT Faint Standards Fundamental and Extended Lists.

Name	RA (J2000)	Dec	K		$J - H$		$H - K$	
FS 101	00 13 43.58	+30 37 59.9	10.384 (0.006)	[8]	0.139 (0.004)	[8]	0.032 (0.003)	[8]
FS 102	00 24 28.50	+07 49 00.1	11.218 (0.005)	[6]	0.318 (0.005)	[7]	0.052 (0.002)	[6]
FS 1	00 33 54.48	−12 07 58.1	12.964 (0.004)	[9]	0.387 (0.003)	[10]	0.057 (0.004)	[9]
FS 103	00 36 29.60	+37 42 54.3	11.731 (0.006)	[6]	0.515 (0.003)	[6]	0.084 (0.006)	[6]
FS 2	00 55 09.93	+00 43 13.1	10.472 (0.004)	[12]	0.206 (0.003)	[11]	0.035 (0.002)	[12]
FS 3	01 04 21.63	+04 13 36.0	12.823 (0.003)	[7]	−0.111 (0.003)	[7]	−0.089 (0.005)	[8]
FS 104	01 04 59.43	+41 06 30.8	10.409 (0.005)	[7]	0.101 (0.004)	[7]	0.026 (0.002)	[7]
FS 105	01 19 08.19	+07 34 11.5	10.970 (0.004)	[6]	0.471 (0.008)	[6]	0.080 (0.001)	[6]
FS 106	01 49 46.94	+48 37 53.2	11.759 (0.005)	[5]	0.616 (0.005)	[6]	0.103 (0.006)	[5]
FS 107	01 54 10.14	+45 50 38.0	10.231 (0.015)	[3]	0.213 (0.010)	[3]	0.050 (0.004)	[3]
FS 5	01 54 34.65	−06 46 00.4	12.339 (0.005)	[8]	0.004 (0.002)	[7]	−0.005 (0.002)	[8]
FS 4	01 54 37.70	+00 43 00.5	10.284 (0.002)	[11]	0.239 (0.004)	[11]	0.032 (0.002)	[11]
FS 6	02 30 16.64	+05 15 51.1	13.382 (0.005)	[8]	−0.059 (0.005)	[8]	−0.069 (0.005)	[8]
FS 7	02 57 21.21	+00 18 38.2	10.945 (0.002)	[14]	0.126 (0.002)	[14]	0.032 (0.001)	[14]
FS 108	03 01 09.85	+46 58 47.7	9.731 (0.004)	[5]	0.290 (0.004)	[5]	0.059 (0.003)	[6]
FS 109	03 13 24.16	+18 49 38.4	10.807 (0.006)	[6]	0.464 (0.005)	[7]	0.161 (0.004)	[7]
FS 110	03 41 02.22	+06 56 15.9	11.324 (0.003)	[6]	0.308 (0.002)	[7]	0.078 (0.004)	[7]
FS 111	03 41 08.55	+33 09 35.5	10.289 (0.006)	[7]	0.262 (0.006)	[7]	0.089 (0.002)	[7]
FS 112	03 47 40.70	−15 13 14.4	10.899 (0.005)	[6]	0.264 (0.004)	[6]	0.047 (0.005)	[6]
FS 10	03 48 50.20	−00 58 31.2	14.983 (0.011)	[9]	−0.104 (0.006)	[9]	−0.118 (0.010)	[9]
FS 113	04 00 14.07	+53 10 38.5	12.432 (0.005)	[6]	0.372 (0.003)	[6]	0.109 (0.005)	[6]
FS 114	04 19 41.72	+16 45 22.4	13.445 (0.006)	[5]	0.604 (0.002)	[6]	0.337 (0.006)	[5]
FS 115	04 23 18.17	+26 41 16.4	10.171 (0.004)	[6]	1.585 (0.009)	[7]	0.772 (0.004)	[7]
FS 116	04 23 50.18	+26 40 07.7	10.949 (0.002)	[7]	1.261 (0.007)	[6]	0.511 (0.003)	[7]
FS 117	04 23 56.61	+26 36 38.0	10.078 (0.004)	[7]	0.950 (0.008)	[7]	0.437 (0.002)	[7]
FS 118	04 24 33.49	+26 33 37.8	10.446 (0.005)	[6]	0.723 (0.005)	[6]	0.266 (0.001)	[6]
FS 11	04 52 58.92	−00 14 41.6	11.254 (0.002)	[18]	0.065 (0.001)	[18]	0.022 (0.001)	[18]
FS 119	05 02 57.44	−01 46 42.6	9.851 (0.004)	[6]	0.045 (0.006)	[6]	0.019 (0.002)	[6]
FS 12	05 52 27.66	+15 53 14.3	13.916 (0.006)	[13]	−0.115 (0.003)	[13]	−0.094 (0.005)	[13]
FS 13	05 57 07.59	+00 01 11.4	10.140 (0.002)	[12]	0.313 (0.002)	[13]	0.048 (0.001)	[12]
FS 120	06 14 01.44	+15 09 58.3	10.626 (0.006)	[6]	0.503 (0.004)	[7]	0.199 (0.006)	[7]
FS 121	06 59 46.82	−04 54 33.2	11.315 (0.003)	[7]	0.561 (0.003)	[7]	0.108 (0.003)	[7]
FS 122	07 00 52.02	+48 29 24.0	11.338 (0.003)	[7]	0.268 (0.003)	[6]	0.046 (0.003)	[7]
FS 14	07 24 14.40	−00 33 04.1	14.198 (0.008)	[8]	−0.065 (0.007)	[8]	−0.031 (0.010)	[8]
FS 15	08 51 05.81	+11 43 46.9	12.348 (0.003)	[13]	0.337 (0.003)	[13]	0.054 (0.002)	[13]
FS 123	08 51 11.88	+11 45 21.5	10.211 (0.004)	[10]	−0.012 (0.002)	[10]	−0.022 (0.004)	[10]
FS 16	08 51 15.01	+11 49 21.2	12.628 (0.004)	[11]	0.290 (0.003)	[11]	0.041 (0.002)	[11]
FS 17	08 51 19.31	+11 52 10.4	12.274 (0.002)	[10]	0.327 (0.003)	[10]	0.056 (0.002)	[10]
FS 18	08 53 35.51	−00 36 41.7	10.527 (0.002)	[11]	0.252 (0.003)	[11]	0.041 (0.002)	[11]
FS 124	08 54 12.07	−08 04 58.9	10.776 (0.004)	[6]	0.481 (0.006)	[7]	0.266 (0.005)	[7]
FS 125	09 03 20.60	+34 21 03.9	10.374 (0.005)	[10]	0.376 (0.002)	[9]	0.052 (0.003)	[10]
FS 126	09 19 18.73	+10 55 54.2	11.680 (0.005)	[10]	0.564 (0.003)	[10]	0.105 (0.003)	[9]
FS 127	10 06 29.03	+41 01 26.6	11.654 (0.004)	[10]	0.261 (0.004)	[9]	0.040 (0.003)	[10]
FS 19	10 33 42.75	−11 41 38.3	13.782 (0.006)	[9]	−0.085 (0.005)	[9]	−0.115 (0.007)	[9]
FS 128	11 05 10.40	+07 06 48.7	12.078 (0.004)	[5]	0.616 (0.003)	[5]	0.309 (0.005)	[6]
FS 20	11 07 59.93	−05 09 26.1	13.501 (0.010)	[6]	−0.038 (0.006)	[6]	−0.065 (0.008)	[6]
FS 129	11 21 48.95	−13 13 07.9	10.709 (0.006)	[8]	0.724 (0.006)	[8]	0.425 (0.002)	[7]
FS 130	11 24 55.92	+34 44 38.5	12.252 (0.003)	[6]	0.596 (0.006)	[7]	0.099 (0.004)	[6]
FS 21	11 37 05.15	+29 47 58.4	13.147 (0.002)	[9]	−0.069 (0.004)	[9]	−0.090 (0.004)	[9]
FS 131	12 14 25.40	+35 35 55.6	11.314 (0.005)	[5]	0.259 (0.003)	[6]	0.032 (0.004)	[5]

Table 4 – *continued*

Name	RA (J2000)	Dec	<i>K</i>	<i>J-H</i>	<i>H-K</i>
FS 132	12 21 39.36	−00 07 13.3	11.836 (0.004) [6]	0.290 (0.003) [7]	0.034 (0.005) [6]
FS 33	12 57 02.30	+22 01 52.8	14.254 (0.005) [6]	−0.112 (0.002) [5]	−0.103 (0.008) [5]
FS 133	13 15 52.80	+46 06 36.9	11.877 (0.004) [5]	0.367 (0.005) [5]	0.060 (0.003) [4]
FS 23	13 41 43.57	+28 29 49.5	12.375 (0.003) [11]	0.527 (0.003) [11]	0.066 (0.003) [11]
FS 134	14 28 43.37	+33 10 41.5	10.747 (0.004) [6]	0.746 (0.004) [6]	0.424 (0.002) [6]
FS 135	14 40 58.04	−00 27 46.6	11.594 (0.003) [5]	0.344 (0.003) [5]	0.046 (0.002) [6]
FS 136	14 59 32.05	−00 06 17.0	11.883 (0.005) [6]	0.553 (0.004) [6]	0.090 (0.004) [6]
FS 137	16 26 42.72	+05 52 20.3	11.829 (0.006) [5]	0.273 (0.006) [7]	0.045 (0.003) [6]
FS 138	16 28 06.72	+34 58 48.3	10.412 (0.006) [7]	0.030 (0.006) [6]	0.002 (0.002) [7]
FS 139	16 33 52.96	+54 28 22.1	12.103 (0.006) [7]	0.512 (0.006) [7]	0.091 (0.003) [7]
FS 27	16 40 41.56	+36 21 12.4	13.128 (0.005) [10]	0.306 (0.005) [10]	0.048 (0.004) [10]
FS 140	17 13 22.65	−18 53 33.8	10.369 (0.006) [5]	0.369 (0.004) [5]	0.060 (0.005) [5]
FS 141	17 48 58.87	+23 17 43.7	10.812 (0.006) [7]	0.303 (0.004) [7]	0.061 (0.003) [7]
FS 35	18 27 13.52	+04 03 09.4	11.748 (0.005) [14]	0.369 (0.003) [15]	0.084 (0.002) [15]
FS 142	18 29 51.26	+01 13 19.0	13.393 (0.011) [2]	1.495 (0.005) [2]	0.750 (0.006) [2]
FS 143	18 29 53.79	+01 13 29.9	13.018 (0.010) [4]	2.336 (0.011) [3]	1.200 (0.005) [4]
FS 144	18 29 56.90	+01 12 47.1	11.046 (0.001) [2]	2.513 (0.017) [2]	1.302 (0.010) [2]
FS 145	18 30 05.81	+01 13 47.3	12.160 (0.006) [4]	3.234 (0.049) [4]	1.562 (0.009) [4]
FS 146	18 54 04.01	+37 07 18.6	10.141 (0.005) [5]	0.511 (0.005) [5]	0.070 (0.003) [5]
FS 147	19 01 55.27	+42 29 19.6	9.866 (0.004) [4]	0.028 (0.004) [5]	0.015 (0.003) [5]
FS 148	19 41 23.52	−03 50 56.1	9.478 (0.004) [5]	0.020 (0.008) [5]	0.011 (0.005) [5]
FS 149	20 00 39.25	+29 58 40.0	10.086 (0.009) [6]	0.023 (0.008) [6]	−0.003 (0.003) [6]
FS 150	20 36 08.44	+49 38 23.5	9.960 (0.005) [8]	0.154 (0.007) [9]	0.044 (0.003) [9]
FS 34	20 42 34.73	−20 04 34.8	13.000 (0.004) [9]	−0.077 (0.003) [9]	−0.074 (0.005) [9]
FS 151	21 04 14.75	+30 30 21.2	11.876 (0.007) [8]	0.274 (0.006) [8]	0.061 (0.005) [8]
FS 29	21 52 25.36	+02 23 20.7	13.311 (0.003) [11]	−0.068 (0.002) [11]	−0.070 (0.003) [11]
FS 152	22 27 16.12	+19 16 59.2	11.057 (0.005) [9]	0.521 (0.005) [8]	0.062 (0.004) [9]
FS 30	22 41 44.72	+01 12 36.5	12.022 (0.003) [15]	−0.042 (0.002) [13]	−0.031 (0.002) [14]
FS 153	23 02 32.07	−03 58 53.1	10.896 (0.004) [6]	0.580 (0.005) [7]	0.105 (0.002) [7]
FS 31	23 12 21.60	+10 47 04.1	14.037 (0.007) [10]	−0.130 (0.005) [10]	−0.099 (0.005) [10]
FS 32	23 16 12.37	−01 50 34.6	13.676 (0.007) [8]	−0.107 (0.003) [8]	−0.086 (0.005) [8]
FS 154	23 18 10.08	+00 32 55.6	11.064 (0.005) [6]	0.264 (0.003) [7]	0.042 (0.003) [7]
FS 155	23 49 47.82	+34 13 05.1	9.413 (0.006) [6]	0.511 (0.003) [5]	0.085 (0.003) [6]

Notes to Table 4.

- (1) The standard error of the mean is shown in parentheses.
- (2) The number of nights from which IRCAM3 data have been retained are shown in square brackets.
- (3) FS 18 is a double star with separation = $1''.36$, p.a. 96° , $\Delta(K) = 2.^m2$ (Y. Clenet 1999, personal communication).